Magnetism driven by anion vacancies in superconducting α-FeSe$_{1-x}$

K.-W. Lee,[1,2] V. Pardo,[1,3] and W. E. Pickett[1]

[1]*Department of Physics, University of California-Davis, Davis, California 95616, USA*
[2]*Department of Display and Semiconductor Physics, Korea University, Jochiwon, Chungnam 339-700, Republic of Korea*
[3]*Departamento de Fisica Aplicada, Facultad de Fisica, Universidad de Santiago de Compostela, E-15782 Campus Sur s/n, Santiago de Compostela, Spain*

To study the microscopic electronic and magnetic interactions in the substoichiometric iron chalcogenide FeSe$_{1-x}$ which is observed to superconduct at $x \approx \frac{1}{8}$ up to $T_c = 27$ K, we use first principles methods to study the Se vacancy in this nearly magnetic FeSe system. The vacancy forms a ferrimagnetic cluster of eight Fe atoms, which for the ordered $x = \frac{1}{8}$ alloy leads to half-metallic conduction. Similar magnetic clusters are obtained for FeTe$_{1-x}$ and for BaFe$_2$As$_2$ with an As vacancy although neither of these are half-metallic. Based on fixed spin-density results, we suggest the low-energy excitations in FeSe$_{1-x}$ are antiparamagnonlike with short correlation length.

I. INTRODUCTION

The discovery of superconductivity,[1] now up to 55 K in the LaFeAsO class of compounds, followed by T_c of nearly 30 K in the BaFe$_2$As$_2$ class with the same active conducting Fe$_2$As$_2$ layer has caused tremendous excitement. A competition between superconductivity and magnetism is very evident, and the assortment of phenomena, concepts, and proposed models is leading to a wide variety of suggestions that is reminiscent of the heyday of high-temperature superconducting cuprates. There is a serious need to identify and address relatively straightforward questions, in addition to broader investigations to compare and contrast all the $\mathcal{R}$FeAsO materials ($\mathcal{R}$=rare earth) to identify trends that might provide a clue. The system, FeSe, has the same band filling as the superconducting oxypnictides, but having only two atoms is structurally simpler and provides more direct questions. Although many samples are two phase and are not always fully characterized, this system is reported to be nonmagnetic and nonsuperconducting at stoichiometry, and is magnetic and clearly superconducting[2–6] at Se substoichiometry FeSe$_{1-x}$.

FeSe can be substoichiometric on either sublattice and contains two major phases (α and β). The PbO-type α-FeSe$_{1-x}$ compound is the one of current interest and has been studied extensively for its spintronics-related magnetic properties by Shen and co-workers,[7–10] who concluded from observed hysteresis a ferromagnetic (FM) state in the nonstoichiometric phase, but a nonmagnetic state in the stoichiometric phase. Very recently, Hsu *et al.*[2] reported superconductivity with $T_c = 8$ K, at $x = 0.12$ and 0.18. Subsequently, T_c has been raised rapidly up to 27 K at pressure $P = 1.48$ GPa,[3,4] clearly putting FeSe$_{1-x}$ in the high T_c category with iron pnictides having similar band filling. Margadonna *et al.*[4] confirmed $T_c \sim 14$ K at $x = 0.08$ at ambient pressure. Fang *et al.*[5] investigated isovalent Fe(Se$_{1-y}$Te$_y$)$_{0.82}$, finding y-dependent T_c in the range of 8–14 K with maximum at $y \approx 0.6$, dipping to zero at $y = 1$. Notably, temperature-dependent susceptibility measurements show an anomaly around 100 K, indicating a peculiar and not yet understood magnetic instability.[2,5] Hence, the competition between superconductivity and magnetism observed in iron pnictides is clearly extended to these iron chalcogenides, and the current picture seems to be that superconductivity arises in a phase with strong magnetic character. Here we focus on a crucial feature: Se vacancies are necessary for producing the high-temperature superconducting state, so what is the character of this defect?

II. STRUCTURE AND CALCULATION

In the tetragonal phase α-FeSe with PbO (B10) structure (space group: $P4/nmm$, No. 129), Fe and Se atoms lie at $2a$ sites (0,0,0) and at $2c$ sites $(0, \frac{1}{2}, z)$, respectively. The Fe$_2$Se$_2$ layers have the same structure as in LaFeAsO and BaFe$_2$As$_2$. The experimental lattice parameters $a = 3.7693$ Å and $c = 5.4847$ Å, which are reported recently by Hsu *et al.*[2] at $x = 0.12$, are used in our calculations. The internal parameter $z = 0.2372$ is optimized by energy minimization within the local density approximation (LDA).

Since the superconductivity has been observed around $x = 0.12$ at ambient pressure, we have used a 2×2 supercell containing 8 f.u. In this supercell, a Se vacancy represents the $x = 0.125$ phase, well within the superconducting regime. In this phase, this supercell contains two types of Fe atoms, one being adjacent to the Se vacancy (Fe1) and the other farther away (Fe2). As shown in our optimized structure given in Table I, the main effect of the Se vacancy on the structure is to shift Fe1 atoms toward the vacant site, whereas Fe2 atoms are affected little. The changes in interatomic distance are −0.14 Å for Fe1-Fe1, +0.07 Å for Fe1-Fe2, and +0.05 Å for Fe1-Se.

Two all-electron full-potential codes, FPLO-7 (Refs. 11 and 12) and WIEN2K (Ref. 13) based on the augmented plane wave plus local orbitals (APW+lo) method,[14] have been used in these calculations with consistent results. The Brillouin zone was sampled with regular dense mesh containing up to 720 irreducible k points. Using WIEN2K with the Perdew-Wang LDA exchange-correlation functional,[15] the atomic positions in the 2×2 supercell with one Se vacancy

TABLE I. Optimized structure for a 2×2 supercell with a Se vacancy (space group: $P4mm$, No. 99), i.e., Fe_8Se_7. The order of Fe-Fe distances for the relaxed structure is Fe1-Fe1, Fe2-Fe2, and Fe1-Fe2. Fe1 means Fe atoms near a Se vacancy. Note that this structure is optimized in ferromagnetic state.

		Unrelaxed			Relaxed		
		x	y	z	x	y	z
Fe1	$4e$	0	0.25	0	0	0.2520	0.2375
Fe2	$4f$	0.5	0.25	0	0.5	0.2637	0.2350
Se1	$2c$	0.5	0	0.7628	0.5	0	0.9950
Se2	$4d$	0.25	0.25	0.2372	0.2481	0.2481	0.4795
Se3	$1a$	0	0	0.7628	0	0	0.0020
bond		Fe-Se: 2.28			Fe1(Fe2)-Se: 2.33(2.29)		
length (Å)		Fe-Fe: 2.66			Fe-Fe: 2.52, 2.68, 2.73		

were optimized until forces were smaller than 2 mRy/a.u. For WIEN2K, local orbitals were added to gain flexibility in dealing with semicore states, Fe $3p$ and Se $3d4s$. The basis size was determined by $R_{mt}K_{max}=6$. Atomic radii used were 2.21 a.u. for Fe and 1.96 a.u. for Se.

III. RESULTS

A. Stoichiometric phase

All attempts to obtain either FM or antiferromagnetic (AFM) states led only to nonmagnetic (NM) solution once the Se position is optimized. Even in the fixed spin moment calculations, no (meta)stable FM state is obtained. The nonmagnetic ground state at $x=0$ is consistent with experimental observations.[10] Subedi *et al.*[16] reported an AFM ground state with a very small stabilization energy; this result is not in serious conflict since energies and moments in these materials are known to be very sensitive to structural and computational details.[17] We have found such an AF ordering is stable using the generalized gradient approximation, but not with our LDA approach (both with WIEN2K and FPLO). All these results taken together indicate FeSe is very near a magnetic critical point.

As seen in other superconductors containing FeAs layers, a transition from tetragonal to a low-temperature orthorhombic structure has been observed around $T=70$ K.[2,4] As expected from the tiny changes in crystal structures, the calculated change in electronic structures is slight. We will address only the tetragonal phase here.

The main difference in the band structure of FeSe (Ref. 16) with respect to iron-pnictide compounds with similar structure occurs along the Γ-Z line (k_z direction). FeSe has a similar band structure to $BaFe_2As_2$,[18] with a flat band (a d orbital lying in the xy plane with a large Fe-Fe hopping integral) (at -20 meV) just below E_F, whereas this band lies above E_F in LaOFeAs,[17] FeTe,[16] and LiFeAs.[18] As might be expected, the Fermi surfaces shown in Fig. 1 are less two-dimensional in FeSe than in iron-pnictide compounds, which have another layer of atoms between FePn layers.

Figure 2 shows the total density of states for $x=0$ compared with that for $x=0.125$. The density of states $N(E_F)$ for $x=0$ is small, 25% less than the value for LaFeAsO and

providing no tendency for a FM instability. However, there is a van Hove singularity at -50 meV, which is absent in the Fe-As superconductors. A difference compared to Fe-As compounds is the hybridization gap at -3 eV that suggests strong Fe-Se hybridization, consistent with about 5% smaller Fe-Se distance in this compound than Fe-As distance in either LaFeAsO or $BaFe_2As_2$. The Se p states also lie somewhat lower than the As p states.

B. Effect of a Se vacancy

This Se vacancy cannot be treated well by the virtual crystal approximation, which we have confirmed by calculations, thus necessitating a supercell treatment of the actual vacancy. The virtual crystal approximation replaces both Se atoms and the vacancy by a peculiar average entity which artificially restores periodicity. Such a model cannot bear any relation to the defected system we study. For $x=0.125$, we find that a strong magnetic state centered on the vacancy is stabilized (see below). This relaxed magnetic defect, with structure given in Table I, gains 32 meV/Fe by structural relaxation. Disregarding magnetism, both structures (relaxed and unrelaxed) are nearly degenerate. This difference reflects important magnetostructural coupling, as already found for LaFeAsO,[17] and dependence of optimized structure on magnetic states is observed commonly in the FeAs-based superconductors,[19,20] which have large calculated spin moment. In this relaxed structure, the magnetization energy (energy difference between NM and FM) is 133 meV/Fe, one-third larger than in the unrelaxed structure and reflecting a very strongly magnetic cluster.

Now we will address the unusual properties of the magnetic state. The most interesting point is that the two types of Fe ions are aligned antiparallel: Fe1 with $2.14\mu_B$ and Fe2 with $-1.10\mu_B$ in the relaxed structure, which reflects a local AFM coupling (as opposed to a delocalized spin-density wave mechanism). This distribution of Fe d states of each spin can be observed in the atom-projected densities of states given in Fig. 3. The net moment is $0.5\mu_B$/Fe, and in addition this ordered system is half-metallic ($1\mu_B$/Fe pair), as shown clearly in the band structure given in Fig. 4. In the unrelaxed structure each Fe ion has smaller moment in magnitude by
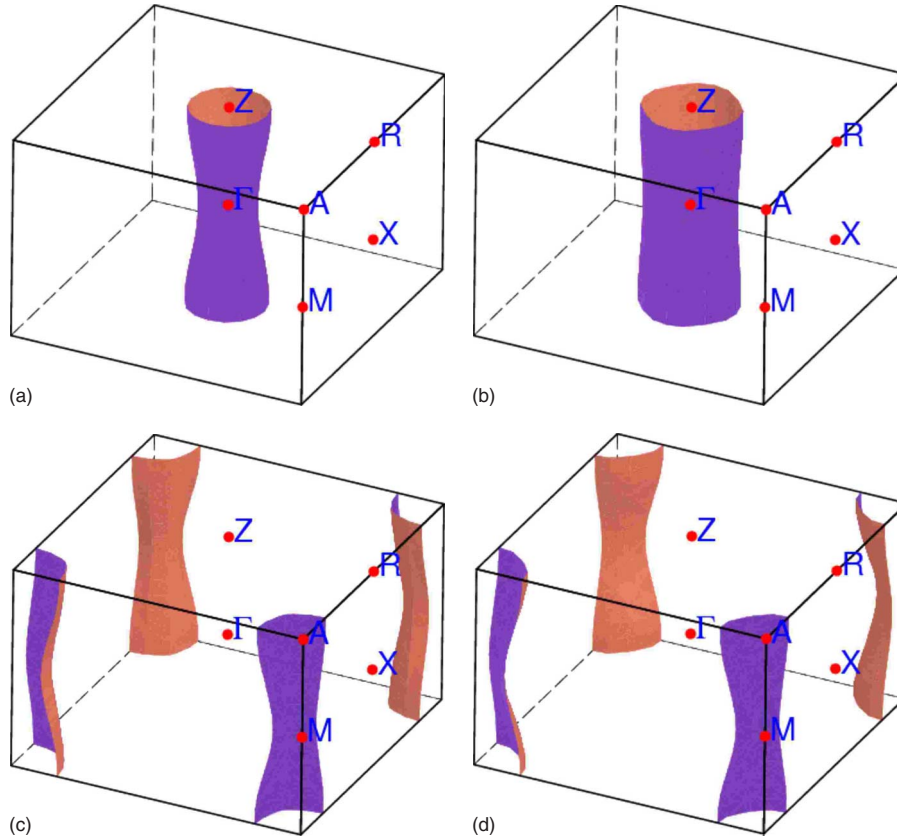
FIG. 1. (Color online) Fermi surfaces (FSs) for nonmagnetic $x=0$ phase. The FSs, consistent with those shown already by Subedi *et al.* (Ref. 16), consist of two Γ-centered hole cylinders, which contain 0.07 and 0.04 holes per a Fe, respectively, and two compensating M-centered electron cylinders with more dispersion along the k_z direction.

$0.25\mu_B$, although the total moment remains unchanged. The Se vacancy leads to creation of antialigned spin moments rather than any identifiable charge difference between Fe ions.

C. Fixed spin moment studies

One may ask: how stable is this antialigned local spin state? Fixed spin moment calculations[21] in the Fe_8Se_7 compound are used to investigate this question. Results can be
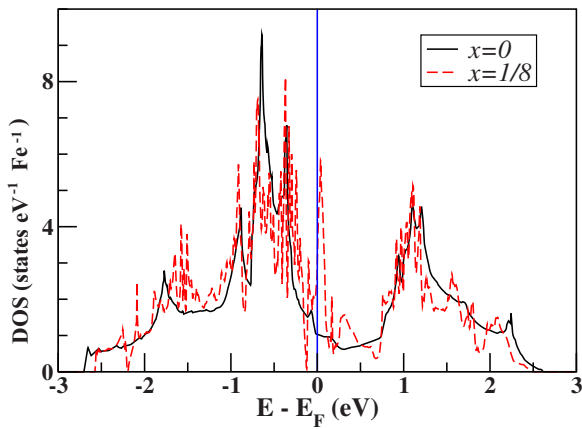

FIG. 2. (Color online) Total densities of states (DOSs) per Fe (both spins), for nonmagnetic $x=0$ and nonmagnetic $x=\frac{1}{8}$ in the optimized structures, in the regime of Fe $3d$ states. Note that the Fermi level E_F of $x=\frac{1}{8}$ lies on steep side of a sharp peak, promoting a stable magnetic state. $N(E_F)$ of $x=\frac{1}{8}$ at E_F is 3.07 states/eV per one Fe, which is about three times larger than that of $x=0$.
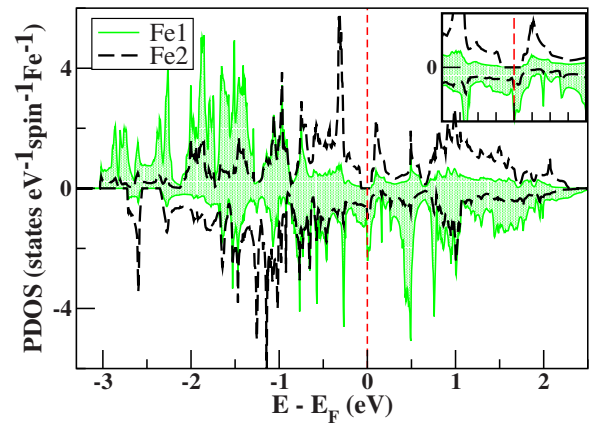

FIG. 3. (Color online) Fe atom-projected densities of state (PDOSs) of magnetic $x=\frac{1}{8}$ in the regime of Fe $3d$ states. The vertical line indicates E_F, set to zero, which passes through a peak in the minority and nearly bisects the gap of ~0.1 eV in the majority. *Inset:* Blowup PDOS in the range of $-0.4-0.4$ eV, clearly showing a gap in the majority channel.
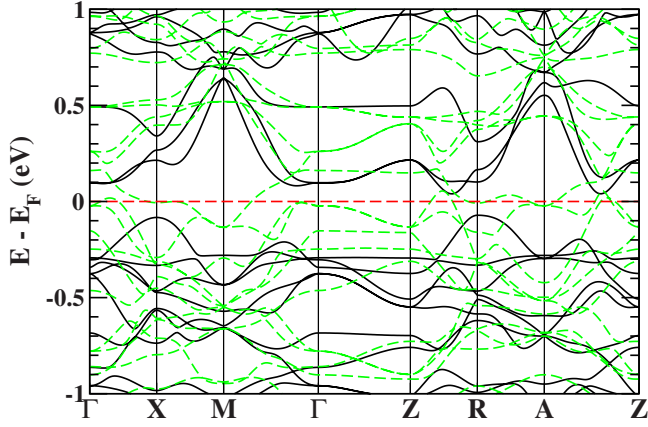
FIG. 4. (Color online) Blowup band structure of magnetic $x=\frac{1}{8}$, showing half-metallicity with total spin moment of $0.5\mu_B$ per Fe, near E_F which is set to zero.
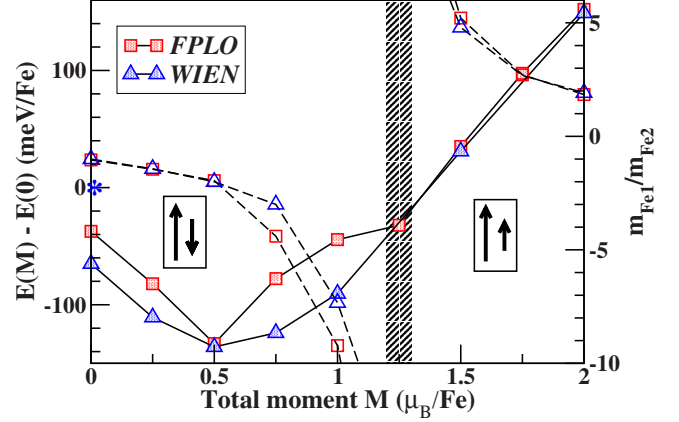

FIG. 5. (Color online) Total energy differences (solid lines, scale on the left axis) and ratio of local moments on Fe ions (dashed lines, scale on the right axis) versus fixed spin moment, using FPLO and WIEN2K. For $M \approx 0.75 - 1\mu_B$, two distinct states can be found. The dashed area is a boundary separating regimes of antiparallel and parallel spin moments (at the boundary, Fe2 has nearly zero moment) described by arrows. The symbol $*$ at $M=0$ denotes nonmagnetic state, which has zero energy $E(0)$ in this plot. The $M=0$ state at -65 meV has compensating moments on Fe1 and Fe2 of magnitude $\sim 1.9\mu_B$. (For details, see text.)

seen in Fig. 5, which shows the expected energy minimum around the half-metallic solution with $0.5\mu_B/$Fe ($4\mu_B$ per magnetic cluster). Note that the $E(M)$ curve is not smooth at a point of half-metallicity[22] where a substantial range of "applied field" leads to the same unchanging moment. For total moment $M=0$, two solutions are found: the antialigned spin state with net zero moment and the simple nonmagnetic state. The antialigned state has lower energy by 65 (37 in FPLO) meV/Fe than the nonmagnetic state, but higher energy by 71 meV/Fe than the half-metallic state. However, the nonmagnetic solution is more stable than any solution with parallel aligned spins. These results indicate that parallel spins are strongly antagonistic for this magnetic cluster; the local coupling is AFM.

For antialigned spin states, the difference in total energy between the two codes used here is associated with different local moments on Fe ions. These differences between two all-electron full-potential codes, which usually give equivalent results, reaffirm the strong sensitivity of the system to small effects. At $M=0$ and $0.25\mu_B$, the moment of Fe1 obtained in WIEN2K is about 15% larger than in FPLO, though

the ratio of Fe local moments is nearly identical. These differences probably reflect the sensitivity of $FeSe_{1-x}$—the softness of its magnetism—to small computational details rather than representing distinct magnetic states. Additionally, changing the total moment for the antialigned spin states, the Fe1 moment is insensitive, with only a maximum change of 10%, whereas the Fe2 moment varies rapidly. From such behavior we can conclude that low-energy excitations involve essentially little change in the Fe1 magnetic moment.

D. Analogies in $BaFe_2As_2$ and FeTe

To check the robustness of this vacancy induced magnetic cluster, we carried out analogous calculations for $FeTe_{1-x}$

TABLE II. Optimized structure for a 2×2 supercell with an As vacancy (space group: $P4/mmm$, No. 123), i.e., $Ba_4Fe_8As_7$, in ferromagnetic state. The lattice parameters (Ref. 24) $a=3.9625$ Å and $c=12.0168$ Å were used for the optimization. In addition to atoms given below, Ba atoms lie at $1a$ site $(0,0,0)$, $1c$ site $(\frac{1}{2},\frac{1}{2},0)$, and $2f$ sites $(0,\frac{1}{2},0)$. The order of Fe-Fe distances for the relaxed structure is Fe1-Fe1, Fe2-Fe2, and Fe1-Fe2. Fe1 means Fe atoms near an As vacancy.

		Unrelaxed			Relaxed		
		x	y	z	x	y	z
Fe1	$8s$	0	0.25	0.25	0	0.2277	0.2561
Fe2	$8t$	0.25	0.5	0.25	0.2506	0.5	0.2522
As1	$4i$	0	0.5	0.6455	0	0.5	0.6556
As2	$2h$	0.5	0.5	0.6455	0.5	0.5	0.6536
As3	$8r$	0.25	0.25	0.1455	0.2526	0.2526	0.1569
Ba	$4k$	0.25	0.25	0.5	0.2548	0.2548	0.5
bond		Fe-As: 2.40			Fe1(Fe2)-As: 2.42 (2.32)		
length (Å)		Fe-Fe: 2.80			Fe-Fe: 2.55, 2.80, 2.93		

and $BaFe_2As_2$. A similar structural relaxation was performed for $FeTe_{0.875}$ as in $FeSe$,[23] and an As vacancy in $BaFe_2As_2$, i.e., $Ba_4Fe_8As_7$ given in Table II. For $BaFe_2As_{1.75}$ and $FeTe_{0.875}$, the relaxation and magnetic cluster are similar although the final states are not half-metallic, with total moment of $0.7\mu_B/Fe$ and $0.42\mu_B/Fe$, respectively. These magnetic states are favored energetically over the nonmagnetic state by about 160 meV/Fe for $BaFe_2As_{1.75}$ and 175 meV/Fe for $FeTe_{0.875}$.

IV. DISCUSSION AND SUMMARY

Now we consider the broader context. Magnetism in superconducting samples, and its possible connection to superconductivity, is one of the primary issues in iron-pnictide superconductivity, and our calculations establish that Se (or Te, or As) vacancies promote strong magnetic clusters surrounding the vacancy. Superconductivity occurs only in substoichiometric samples, and we obtain strong magnetic behavior only around Se vacancies. Our fixed spin moment results indicate the low-energy excitations will involve fluctuations in the magnitude of the next-neighbor Fe spin (relative to the vacancy), while the near-neighbor spin remains rigid and antialigned. The character of this excitation is antiparamagonlike but with short correlation length, a scenario that also seems relevant for the iron-pnictide superconductors.

In the superconducting $FeSe_{0.88}$ materials there is a magnetic transition characterized by a sharp upturn in the susceptibility (apparently also with a structural aspect) near 105 K, followed by another transition at 75 K where the susceptibility abruptly returns to its higher temperature value.[2,5] These anomalies have not been discussed much yet, but the strong magnetic character and the difference in field-cooled and zero-field-cooled susceptibility at lower temperature may be reflecting complex cluster-glass behavior arising from the immobile but interacting magnetic defects that we have studied. The appearance of superconductivity in a disordered magnetic system such as this provides strong justification for further study of the physics of the $FeSe_{1-x}$ system.

[1] Y. Kamihara, T. Watanabe, M. Hirano, and H. Hosono, J. Am. Chem. Soc. **130**, 3296 (2008).

[2] F.-C. Hsu, J.-Y. Luo, K.-W. Yeh, T.-K. Chen, T.-W. Huang, P. M. Wu, Y.-C. Lee, Y.-L. Huang, Y.-Y. Chu, D.-C. Yan, and M.-K. Wu, arXiv:0807.2369 (unpublished).

[3] Y. Mizuguchi, F. Tomioka, S. Tsuda, T. Yamaguchi, and Y. Takano, Appl. Phys. Lett. **93**, 152505 (2008).

[4] S. Margadonna, Y. Takabayashi, M. T. McDonald, K. Kasperkiewicz, Y. Mizuguchi, Y. Takano, A. N. Fitch, E. Suard, and K. Prassides, arXiv:0807.4610, Chem. Commun. (Cambridge) (to be published).

[5] M. H. Fang, L. Spinus, B. Qian, H. M. Pham, T. J. Liu, E. K. Vehstedt, Y. Liu, and Z. Q. Mao, arXiv:0807.4775 (unpublished).

[6] K.-W. Yeh, T.-W. Huang, Y.-L. Huang, T.-K. Chen, F.-C. Hsu, P. M. Wu, Y.-Y. Chu, C.-L. Chen, J.-Y. Luo, D.-C. Yan, and M.-K. Wu, arXiv:0808.0474 (unpublished).

[7] Q. J. Feng, D. Z. Shen, J. Y. Zhang, B. S. Li, B. H. Li, Y. M. Lu, X. W. Fan, and H. W. Liang, Appl. Phys. Lett. **88**, 012505 (2006).

[8] K. W. Liu, J. Y. Zhang, D. Z. Shen, C. X. Shan, B. H. Li, Y. M. Lu, and X. W. Fan, Appl. Phys. Lett. **90**, 262503 (2007).

[9] X. J. Wu, D. Z. Shen, Z. Z. Zhang, J. Y. Zhang, K. W. Liu, B. H. Li, Y. M. Lu, B. Yao, D. X. Zhao, B. S. Li, C. X. Shan, and X. W. Fan, Appl. Phys. Lett. **90**, 112105 (2007).

[10] X. J. Wu, Z. Z. Zhang, J. Y. Zhang, B. H. Li, Z. G. Ju, Y. M. Lu, B. S. Li, and D. Z. Shen, J. Appl. Phys. **103**, 113501 (2008).

[11] K. Koepernik and H. Eschrig, Phys. Rev. B **59**, 1743 (1999).

[12] FPLO-5 has been used partially to consider the virtual crystal approximation (VCA) that has not been implemented in FPLO-7, yet. Valence orbitals included Fe $3s3p4s4p3d$ and Se $3p4s4p3d$ in FPLO-5.

[13] K. Schwarz and P. Blaha, Comput. Mater. Sci. **28**, 259 (2003).

[14] E. Sjöstedt, L. Nordström, and D. J. Singh, Solid State Commun. **114**, 15 (2000).

[15] J. P. Perdew and Y. Wang, Phys. Rev. B **45**, 13244 (1992).

[16] A. Subedi, L. Zhang, D. J. Singh, and M. H. Du, Phys. Rev. B **78**, 134514 (2008).

[17] Z. P. Yin, S. Lebègue, M. J. Han, B. P. Neal, S. Y. Savrasov, and W. E. Pickett, Phys. Rev. Lett. **101**, 047001 (2008).

[18] D. J. Singh, Phys. Rev. B **78**, 094511 (2008).

[19] I. I. Mazin and M. D. Johannes, arXiv:0807.3737 (unpublished).

[20] T. Yildirim, arXiv:0807.3936 (unpublished).

[21] K. Schwarz and P. Mohn, J. Phys. F: Met. Phys. **14**, L129 (1984).

[22] K.-W. Lee and W. E. Pickett, Phys. Rev. B **77**, 115101 (2008).

[23] The experimental lattice parameters (Ref. 6) $a=3.819$ Å and $c=6.250$ Å were used.

[24] M. Rotter, M. Tegel, D. Johrendt, I. Schellenberg, W. Hermes, and R. Pöttgen, Phys. Rev. B **78**, 020503(R) (2008).